University of Tennessee, Knoxville
Trace: Tennessee Research and Creative Exchange

Masters Theses   Graduate School

5-2014

Long-Term Evaluation of Norris Reservoir Operation Under Climate Change

Joseph Patton Rungee II
University of Tennessee - Knoxville, jrungee@utk.edu

Recommended Citation

To the Graduate Council:

I am submitting herewith a thesis written by Joseph Patton Rungee II entitled "Long-Term Evaluation of Norris Reservoir Operation Under Climate Change." I have examined the final electronic copy of this thesis for form and content and recommend that it be accepted in partial fulfillment of the requirements for the degree of Master of Science, with a major in Environmental Engineering.

<div align="right">Ungtae Kim, John S. Schwartz, Major Professor</div>

We have read this thesis and recommend its acceptance:

Chris Cox, Jon Hathaway

<div align="right">Accepted for the Council:
<u>Dixie L. Thompson</u></div>

<div align="right">Vice Provost and Dean of the Graduate School</div>

(Original signatures are on file with official student records.)

Long-Term Evaluation of
Norris Reservoir Operation Under
Climate Change

A Thesis Presented for the
Master of Science
Degree
The University of Tennessee, Knoxville

Joseph Patton Rungee II
May 2014

ACKNOWLEDGEMENTS

ABSTRACT

This study aimed to address the potential long-term effects of future climate change on the Tennessee Valley Authority's (TVA's) operation policy for Norris Reservoir. The Community Earth System Model 1.0 (CESM1.0), a general circulation model (GCM) accessible through the Intergovernmental Panel on Climate Change's (IPCC's) Coupled Model Intercomparison Project Phase 5 (CMIP5), with the Representative Concentration Pathway 4.5 (RCP4.5) was used to obtain projected precipitation and temperature data for three future climate scenarios, 2030's, 2050's, and 2070's. Three hydrologic models were individually calibrated on 30 years of observed runoff data and combined utilizing linear programming to consider the strengths of each model. Inflow hydrographs were simulated for the future time spans using projected precipitation and temperature. Reservoir routing was then simulated using the inflow hydrographs via mass balance and the current operation policy to determine the storage elevation of the reservoir. Next, the routing simulations were utilized as input for a genetic algorithm forced optimization model, to minimize an elevation-based penalty value, optimizing Norris Reservoir's operation policy. Finally, the operation performance of Norris Reservoir's current operation policy versus the policies generated by the developed optimization model for each projected scenario were evaluated. The results suggested a 20.7, 23.8, and 24.3 percent increase in runoff for the 2030's, 2050's, and 2070's, respectively, compared to the BASE case (1976 ~2006). Although the current policy was able to support this increase in runoff, the optimization model decreased operation penalties by 23.3, 22.2, and 24.4 percent for the 2030's, 2050's and 2070's, respectively. These results can provide substantial insight to TVA hydrologists and decision makers that their current policy may require re-evaluation, considering the potential impacts of climate change.

TABLE OF CONTENTS

LIST OF TABLES

LIST OF FIGURES

CHAPTER I

INTRODUCTION

As hydro-climatic databases have expanded and confidence in climate models have increased, professional climatology researchers have consistently concluded that climate change will impact to water resource infrastructure (Frederick and Major 1997, IPCC 2013). Furthermore, the Intergovernmental Panel on Climate Change's (IPCC) Fifth Assessment Report (AR5) states that the period from 1983-2012 has likely been the warmest 30-year period in the past 1400 years, and that there has been a linear trend of the globally averaged combined land and ocean temperature increasing 0.85 °C since 1880 (IPCC 2013). Studies have also shown that climate change has increased the probability of occurrence for extreme climatic events (Allen and Ingram 2002, Bell et al. 2004, Gao et al. 2012, WMO 2013, IPCC 2013). The southeastern United States has experienced increases in moderate to extreme summer droughts since the 1970's and annual average autumn precipitation since 1901 by 14 and 30 percent, respectively (Karl et al. 2009). Due to these increases, major infrastructure concerns regarding water supply and reservoir proficiency (flood and reservoir failure prevention, hydroelectric generation, transportation, etc.) have become apparent (Christensen et al. 2004, Payne et al. 2004, Helton et al. 2006, Choi 2011).

Developing new reservoir management strategies and modelling tools necessary for maintaining water resources and hydro power generation, considering the possible implications of future climate change, has become an high priority research topic (Askew 1987, Arnell 1999, Markoff and Cullen 2007, Guegan et al. 2012). As of late, studies on the Columbia (Hamlet and Lettenmaier 1999, Lee et al. 2009), Colorado (Christensen et al. 2004), and Missouri (Stone et al. 2001) river basins have been conducted which assess the vulnerability and fragility of many current operation policies when analyzed against possible future climate scenarios. Although

studies are being performed in many of the large river basins in the United States, assessments of the impact that climate change for the Tennessee River Basin have been limited (Choi 2011).

Norris Reservoir is the largest reservoir on any tributary of the Tennessee River, and is operated by the Tennessee Valley Authority (TVA) (TVA 2014). In 2004, TVA performed a Reservoir Operation Study (ROS) encompassing 35 of the 49 reservoirs in their system, to determine if modifications to their current policy could increase reservoir efficiency and, "produce greater overall public value" (TVA 2004, TVA 2006). From the ROS, TVA designed a new policy considering multiple objectives including reservoir stability, hydropower generation, cooling requirements for TVA nuclear and fossil facilities, flood control, and navigation (TVA 2004). TVA has simplified these objective into maintaining dam elevation between two curves noted as 'balancing guide' and 'flood guide'. The balancing guide line ensures that all tributary reservoirs are drawn from equally when meeting downstream requirements, whereas the flood guide line represents the maximum amount of storage to help reduce flood damage; it is TVA's objective to maintain reservoir elevation at the flood guide line (TVA 2004, TVA 2014). More importantly, this policy integrates the entire TVA reservoir system into a single network. Providing the ability to systematically optimize all of the reservoirs in an attempt to maintain individual reservoir elevations and based upon outflow requirements to meet a hierarchy of operational demands. However, this new policy must remain adaptable to shifts in environmental factors, such as future climate and land use change.

General Circulation Models (GCM) have been used to project future impacts of climate change on the hydrologic cycle. IPCC's Coupled Model Intercomparison Project Phase 5 (CMIP5), developed in 2010, introduced four new Representative Concentration Pathway (RCP) scenarios (Moss et al. 2010, Wu et al. 2014). Instead of relying simply on greenhouse gas (GHG)

emission scenarios, RCPs account for GHGs, aerosols, chemically active gases, and land use/ land cover. The advantage to the RCP scenario is that it represents a variety of 21st century climate policies, whereas the Special Report on Emission Scenarios (SRES) of the Third and Fourth Assessment Report represented no-climate policy scenarios (IPCC 2013). The four RCP scenarios include RCP2.6, RCP4.5, RCP6.0, and RCP8.5, which represent one of many instances leading to the specific radiative forcing of 2.6, 4.5, 6.0, and 8.5 watts per square meter ($W \cdot m^{-2}$) by the year 2100, respectively (IPCC 2013). More specifically, RCP2.6 is considered a mitigation scenario where radiative forcing peaks at a value of 3.0 $W\ m^{-2}$, and drops to 2.5 $W\ m^{-2}$ by 2100; RCP4.5 is a stabilization scenario which peaks and stabilizes at 4.5 $W\ m^{-2}$ by 2100; RCP6.0 is a stabilization scenario which does not peak at 6.0 $W\ m^{-2}$ by 2100, but is approaching stabilization; and RCP8.5 is a high GHG scenario which does peak a 8.5 $W\ m^{-2}$ at 2100 (Moss et al. 2010, IPCC 2013).

Utilizing TVA's 2004 operation policy for the Norris Reservoir as a case study, this study aims to analyze its performance based on a defined set of optimization routine penalty weights, for its ability to meet the hierarchy of operational demands given the potential impacts of climate change. This is to be accomplished through the utilization of an IPCC CMIP5 RCP4.5 model, due to RCP4.5 being considered a stabilization scenario with the introduction of climate change mitigating policies, to develop three 30 year spans averaging to 2030, 2050, and 2070, noted as 2030's, 2050's, and 2070's, respectively. The overall goal of this study can be achieved from completing four primary objectives:

1. Acquire necessary input data sets for hydrological model calibration and reservoir operation optimization model. This objective is achieved through a combination of collaborating with TVA to obtain Norris Reservoir operating constraints, accessing the National Oceanic and Atmospheric Administration's (NOAA) National Climate Data

Center (NCDC) to procure historically observed data relevant to the study area, and obtaining GCM output data from IPCC's CMIP5 database.

2. Successfully develop and calibrate a combined hydrological model with the ability to simulate runoff for the study area, with high confidence.

3. Simulate runoff for the scenario conditions using the calibrated model with temperature and precipitation inputs obtained from GCM simulations.

4. Develop an optimization model which uses the combined model output as input to simulate reservoir routing. The routing will be evaluated using the current routing policy and then optimized to best meet the hierarchy of TVA defined outflow objectives.

5. Complete an evaluation of Norris Reservoir's current operation policy under future climate scenarios. This will be completed utilizing the optimization model and minimizing penalties (defined by Norris Reservoir's operation constraints) to assess whether TVA's operational objectives can be met under conditions of climate change.

CHAPTER II

MATERIALS AND METHODS

Study Area

Norris Reservoir serves as the primary reservoir for the Powell (Hydrologic Unit Code (HUC: 06010206) and Upper Clinch (HUC: 06010205) River Basins. The coordinate range of the combined Upper Clinch and Powell river basins are approximately (-84.38, 37.23) to (-81.37, 36.23), and their areas are 5124.58 and 2435.34 km^2, respectively. The entire study area, including both basins, location of Norris Reservoir, and metrological stations used can be found in Figure 1.
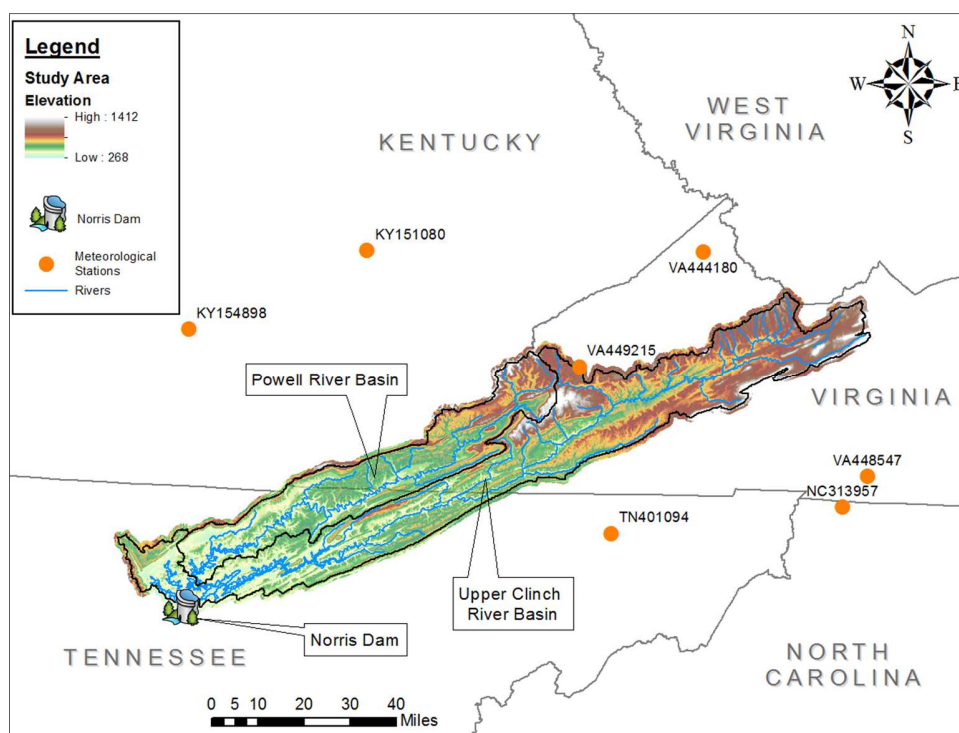
Figure 1. Study Area

Norris Dam (Appendix 1) lies about 482.80 km southwest from the head waters of the Upper Clinch River in Southwest Virginia, and discharges into the Lower Clinch River in Northeast Tennessee. It has a height and length of 80.77 and 566.93 meters, respectively (TVA 2006, TVA 2014). Norris reservoir's primary purposes include hydroelectric power generation, and flood control. It has the flood storage capacity of 1372.87 MCM (million cubic meter), and can generate up to 110 MW (TVA 2014). The impounded water behind the Norris Dam (Norris Lake) has 1301.96 km of shoreline and 13.35 hectares of water surface area, making it the largest reservoir on a Tennessee River tributary (TVA 2014).

Climate and Hydrology

Climate and hydrologic information utilized herein was collected for the study area which, consisting of the Upper Clinch and Powell River Basins, encompasses in parts of northeast Tennessee, southeast Kentucky, and southwest Virginia. The climate for this area is described as humid subtropical, consisting of hot, humid summers and mild winters (Parker 2008, Choi 2011). NCDC observed data dating from January 1, 1976 to December 31, 2006, showed average monthly precipitation and temperature for the study area of 90.62 mm and 13.08°C ranging from 62.00 to 114.60 mm and 1.38 to 23.84 °C, respectively.

The Upper Clinch River has a flow length of 482.80 km with its headwater located just north of Tazwell, Virginia (TDEC 2007, USGS 2013). Further downstream, the Clinch River merges with the Powell River. It is then twice dammed, first by Norris Reservoir, then Melton Hill Reservoir before discharging into the Tennessee River in Kingston, Tennessee. The Powell River's headwater is located in Wise County, Virginia. It then flows 193.1 km, before discharging into the Clinch River (EPA 2002, TDEC 2007). Both the Clinch and Powell rivers flow

southwesterly through parallel valleys and are contained within the Cumberland (Appalachian) Plateau and the Valley and Ridge physiographic provinces (EPA 2002).

Model Input

Operation Policy

The current operation policy for Norris Reservoir was required to effectively evaluate its robustness, understanding that climate change is associated with the non-stationarity of hydro-climatic variables. Since all reservoirs in the TVA system operate as a network to maintain a form of equilibrium, Norris Reservoir's operational priorities are subject to change depending on any single event occurring throughout the system. TVA provided the current Elevation Operating Guide (Figure 2), the minimum flows required for the ecosystem, hydroelectric power generation, and Bull Run fossil plant, the maximum flow to prevent flooding, the historical maximum elevation and elevation which compromises dam safety, and the minimum elevation for reservoir maintenance and elevation required to provide flow for navigation. Therefore, as a case study, the criterion obtained from TVA were believed to be adequate for the development of the routing and optimization model with respect to the scope of this research. In Figure 2, the upper and lower solid turquoise lines represent the Flood Guide and Balancing Guide, respectively. The dashed turquoise line represents the Reservoir Operation Study Median from the 2004 ROS for Norris Reservoir, the black line represents the actual elevation for 2013, and the 80% grey range represents the expected elevation range (TVA 2014).
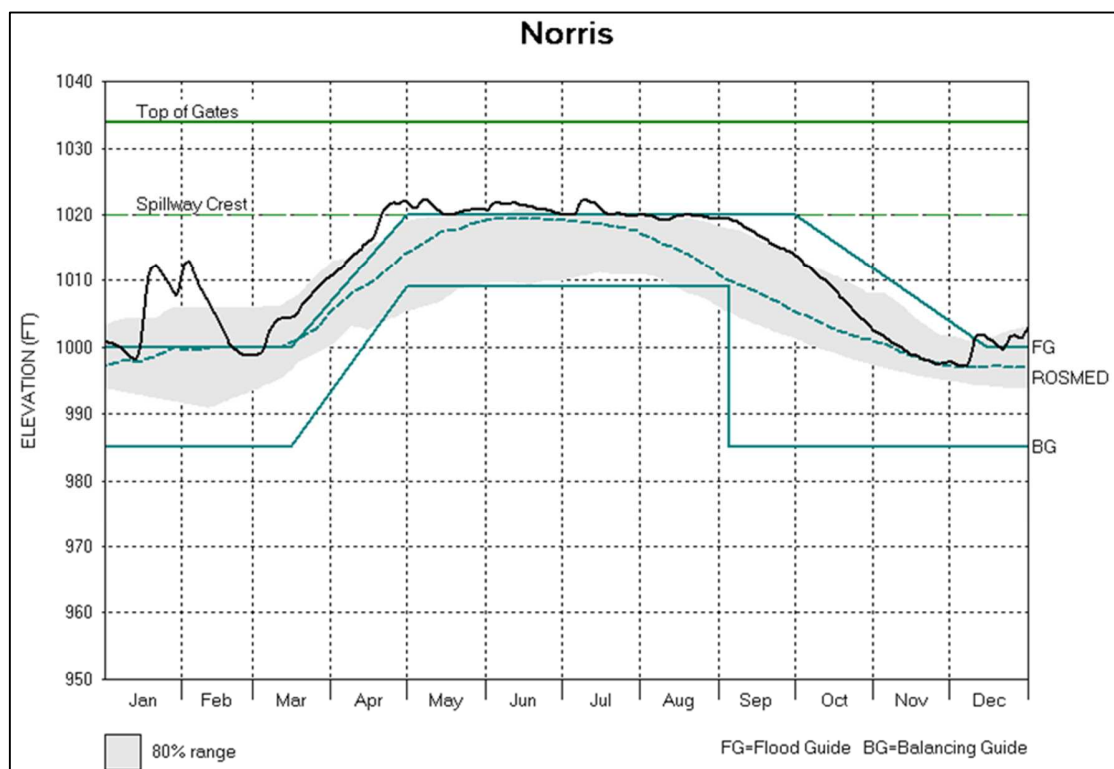
Figure 2. 2013 Norris Reservoir Elevation Guide (Communication with TVA personnel)

Precipitation and Temperature Data

31 years, to account for a previous a time-step, of contiguous and continuous observed precipitation and temperature data were used to calibrate and validate the individual hydrologic models. Based upon this criterion, the five stations selected for precipitation were NC313957, TN401094, VA444180, VA448547, and VA449215. The five stations selected for temperature included KY151080, KY154898, NC313957, TN401094, and VA444180. The stations selected were based upon a recent study that concluded stations with similar latitude and insignificant perturbation in hydro-climatic variables, could accurately represent the climate for the entire study area. (Choi 2011) (Figure 1). The stations were then verified by obtaining NOAA data from the National Climate Data Center (NCDC) confirming that the required criterion of at least 31

contiguous and continuous years for calibration were met. It was determined that the most recent time frame acceptable for calibration was January 1, 1976 to December 31, 2006. The meteorological stations were interpolated via the Thiessen polygon method to determine a representative composite precipitation and temperature value for the study area. This method creates an areal weight for a network of meteorological stations by drawing polygons whose sides are the perpendicular bisectors of lines connecting the gauges (Haan et al. 1994, Kim et al. 2008). Buytaert et al. (2006) confirmed that this method still produced good results given study areas located in mountainous regions. The Theissen polygons were constructed utilizing ESRI's ArcGIS 10.2 software.

Streamflow Data

Observed streamflow data for the inflow to Norris Reservoir was obtained through direct correspondence with TVA personnel. The data were given in units of inches on a monthly time-step dating from January 1921 to February 2013. The data were converted to millimeters for model calibration.

Potential Evapotranspiration

Potential evapotranspiration (PET) was calculated via the Thornthwaite method (Thornthwaite 1948, Palmer and Havens1958, McCabe and Wolock 1992, Lu et al. 2005). The Thornthwaite method is a temperature-based model given by:

$$PET = 1.62b\left(\frac{10mt}{I}\right)^{a} * 10 \qquad (1)$$

where PET is given in millimeters (mm), b is the sunshine hour adjustment for each month (multiples of 12 hours), mt is the monthly mean air temperature (°C), I is the annual heat index,

and $a = 6.75 * 10^{-7}I^3 - 7.71 * 10^{-6}I^2 + 0.01791I + 0.49239$ (Palmer and Havens 1958, Lu et al. 2005, Black 2007).

Hydrologic Rainfall-Runoff Models

For this study, a conceptual, linearly programmed combined model approach was used to construct the combined model from three individual hydrologic models. The individual models used were a multiple linear regression (MLR), an artificial neural network (ANN), and the Tank model. Through linear programming, each individual model was assigned a single weight, which summed to 1. This was performed by minimizing the natural log transformation of the sum square error (LNSSE) from the combined model to the observed data.

Multiple Linear Regression Model (MLR)

Multiple linear regression was both as an individual hydrologic model, and as a means of determining which hydro-climatic variables would be significant in estimating runoff (Table 1). The general expression for MLR is given by Kim and Kaluarachchi (2008):

$$y = \beta_0 + \beta_1 X_1 + \beta_2 X_2 + \cdots + \beta_n X_n \qquad (2)$$

where, β_n is the matrix of regression coefficients of parameter y, and X_n is the matrix of selected variables corresponding to the parameter. In the first step, a multiple linear regression was performed by including only the most influential variable. Subsequently, a "step forward" is taken by including the next most influential variable into the regression. This process continues until either all the variables have been included, or the regression is no longer improved by the addition of a variable (Muleta and Nicklow 2005, Parajka et al. 2005, Helton et al. 2006, Heuvelmans et al.

2006, Wagener and Wheater 2006, Boughton and Chiew 2007, Seelbach et al. 2011). The model was performed utilizing the statistical toolbox in MATLAB.

Table 1. Potential Variable for Combined Model

No.	Symbol	Definition	Unit
1	P_t	Precipitation at time t	mm
2	P_{t-1}	Precipitation at time t-1	mm
3	PET_t	Potential Evapotranspiration at time t	mm
4	PET_{t-1}	Potential Evapotranspiration at time t-1	mm

Artificial Neural Networks Model (ANN)

ANNs have become a widely accepted method by 'neurohydrologists' for estimating rainfall-runoff processes due to the similarities in ANNs and the hydrologic process being considered 'black-box' systems (Dawson and Wilby 2001). ANNs are defined as an information-processing system consisting of many non-linear and densely interconnected neurons or nodes (Tokar and Johnson 1999, Dawson and Wilby 2001). ANNs were developed as a means of mimicking the biological nervous system, in the fact that they have the ability to generate an output based on input parameters regardless of prior knowledge of regularities, noisiness, distortion, or incompleteness of the input data (Zealand et. al, 1999). Figure 3 represents the typical structure of an ANN consisting of three layers: input, hidden, and output (Zealand et al. 1999).
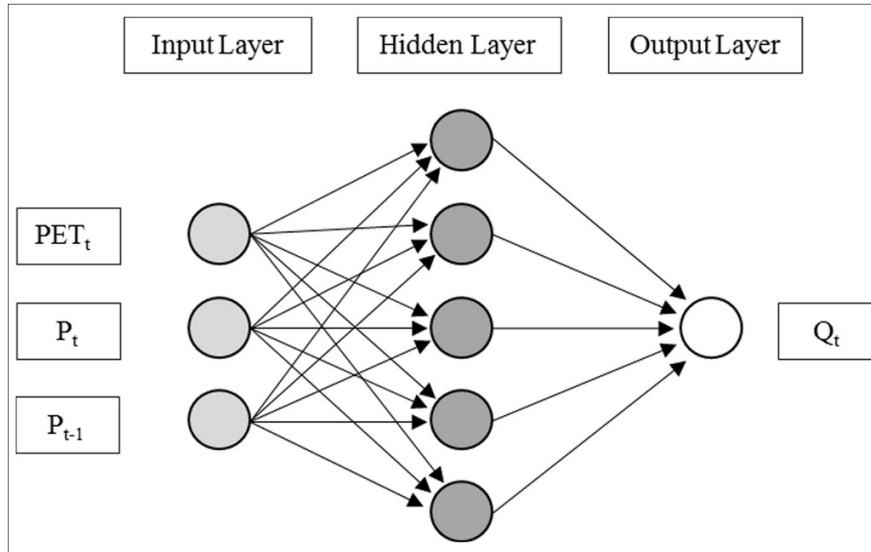
Figure 3. Artificial Neural Network Structure for Hydrological System

The hidden layer, which processes a set number of nodes defined by the user, received its name for the values within the layer being 'unrelated' to the inputs/outputs. This allows for more complex functions to be modelled. The optimum number of nodes required to receive the best output can be derived from a number of methods such as pruning algorithms, cascade correlations, trial and error, etc. (Dawson and Wilby 2001). Next, the output layer consists of the summation of weighted input values determined by the hidden layer. Once training is complete, the model is validated with the remainder of the dataset not utilized for training.

The ANN is trained through forward and reverse iterations between the output and hidden layers in order to minimize the global error E (Kişi 2007), described in Eq (3).

$$E = \frac{1}{n}\sum_{i=1}^{n} E_n \tag{3}$$

where n = total number of training patterns and E_n = the error for training pattern n, is represented by the equation:

$$E_n = \frac{1}{2}\sum_{j=1}^{m}\left(O_j - T_j\right)^2 \tag{4}$$

where m = number of nodes, O_j = output at node j, and T_j = target output at node j (Kişi 2008). The number of training patterns,n, is dependent on the magnitude of the gradient of performance; unless the number of patterns is explicitly specified, training does not end until the gradient of the performance is less than 10^{-5} (Beale et al. 2014). It should also be noted that only one output and target value existed for this study. There are four training algorithms: back-propagation, conjugate gradient, cascade correlation, and Levenberg-Marquardt (Kişi 2007). To begin training, data were introduced into the network, via the input layer, which can consist of one or more vectors representing one to many variables (precipitation, runoff, etc.) (Tokar and Johnson 1999, Zealand et al. 1999).

For this study, the ANN consisted of one hidden layer with ten nodes determined by trial and error, the Levenberg-Marquardt training method, and the same variables determined significant by the stepwise regression; 90 percent of the dataset ranging from 1976 to 2006 was set aside for calibration, 5 percent for validation, and 5 percent for testing. A 10 node hidden layer was selected based upon the trial and error method due to its common use and being considered the best method in scientific literature (Shamseldin 1997, Shamseldin et al. 1997, Dawson and Wilby 2001). The Levenberg-Marquardt training algorithm was selected based upon an analysis performed by (Kişi 2007), where the Levenberg-Marquardt proved to be more efficient and provided the best runoff projections when compared to the other three training algorithms.

Tank Model

The Tank model, which was initially developed by Sugawra (1967), was utilized in this study due to its relatively simple architecture, ability to simulate low flows well, and applicability being internationally verified for multiple river basins (Jain 1993, Yokoo et al. 2001, Chen et al.

2005, Kim and Kaluarachchi 2008, Choi 2011). From the conclusions drawn by Kim and Kaluarachchi (2008), it was decided that six parameters would be sufficient for representing the dynamics of the study area due to the non-linearity of hydro-climatic variables. A two layer tank model was used, where the first layer represents surface flow, and second layer represents groundwater flow, and infiltration from the second layer represents deeper groundwater flow that does not contribute to runoff for the study basin. A schematic for the two-layer model is shown in Figure 4, along with a description of the parameters.
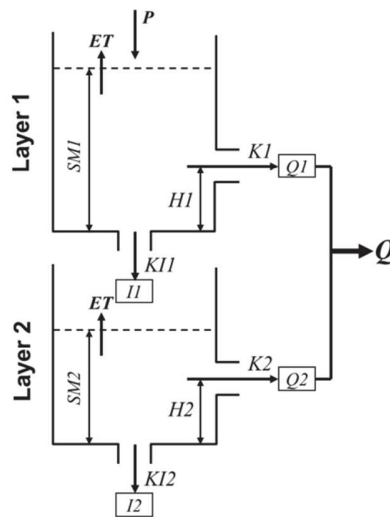
Figure 4. Two-Layer Tank Model Schematic (Kim and Kaluarachchi 2008)

The total runoff, $Q(t)$ in mm, at time t is calculated as:

$$Q(t) = \sum_{i=1}^{n} Q_i(t) \tag{5}$$

where n is the number of layers, and $Q_i(t)$, the runoff for the ith layer at time t, is computed as:

$$Q_i(t) = K_i * (SM_i(t) - H_i) \tag{6}$$
$$for\ H_i < SM_i(t), otherwise\ zero$$

where K_i is the coefficient of runoff for layer i, and H_i is the height of the runoff orifice for layer i, and $SM_i(t)$ represents the soil moisture in mm at time t for layer i computed as:

$$SM_i(t) = SM_i(t-1) + I_{i-1}(t) + \{P(t) - ET_i(t)\} - I_i(t) - Q_i(t) \qquad (7)$$
$$Where\ I_i = 0, for\ i \leq 1;\ and\ P(t) = 0, for\ i > 1$$

where $I_i(t)$ represents the infiltration of the ith layer in mm at time t, and is computed as:

$$I_i(t) = KI_i * SM_i(t-1) \qquad (8)$$

where KI_i is the coefficient of infiltration/percolation, and $SM_i(t-1)$ is the soil moisture at the previous time step for layer i. Due to increased performance in simulating observed hydrographs when compared to other methods (Kim et al. 2008), evapotranspiration at time (t) for the ith layer, $ET_i(t)$ in mm, was approximated via (Dingman 2002):

$$ET_i(t) = \frac{P(t)}{\sqrt{1 + \left(\frac{P(t)}{PET(t)}\right)^2}} \qquad (9)$$

where $P(t)$ is the precipitation in mm at time t, and $PET(t)$ is potential evapotranspiration in mm at time t. After Q_i and all parameters are calculated, $SM_i(t)$ is updated at each time step by calculating the net of layer i. The Tank model was calibrated and validated utilizing a 30 year span of continuous and contiguous precipitation (P) and potential evapotranspiration (PET) data from 1977 to 2006, where the first 20 years were used for calibration, and the remaining 10 were used for validation. The coefficients of runoff (K_i), infiltration/percolation (KI_i), and height of the orifices (H_i) were calibrated using genetic algorithms (GA), which are a renowned form of numerical optimization algorithms used in previous hydrologic studies (Chen et al. 2005, Kim and Kaluarachchi 2008 and 2009, Choi 2011).

Projected Climate Data

Representative Concentration Pathway Scenarios

The Intergovernmental Panel on Climate Change (IPCC) released their Working Group I, Fifth Assessment Report (AR5) in the fall of 2013. This report describes the updates from the previous CMIP versions, with the primary update noted as the use of a new set of scenarios titled Representative Concentration Pathways (RCP). CMIP5 consists of four RCP scenarios, RCP2.6, RCP4.5, RCP6.0, and RCP8.5; where the numerical values correspond with the radiative forcing by the year 2100 (IPCC 2013). For this study, RCP4.5 is the scenario being used due to being a stabilization scenario, assuming that emission mitigation policies will be set in place during the 21st century (Moss et al. 2010, Thomson et al. 2011, Taylor et al. 2012, IPCC 2013, Lee and Wang 2014).

General Circulation Model

GCMs are mathematical models which have become widely used and accepted for simulating future global climate (Elshamy et al. 2009, Choi 2011, Gao et al. 2012, Lee and Wang 2014). CMIP5 has over 60,000 combinations of GCMs and their varying ensembles. A more detailed description for the ensemble members are given in Taylor (2012) and IPCC's AR5 (IPCC 2013). The National Center for Atmospheric Research's (NCAR) Community Earth System Model version 1.0 (CESM1.0) was the GCM chosen for this study due to its use in other research efforts (Gao et al. 2012, Wu et al. 2014). The arithmetic mean of the three ensembles for this models were utilized to minimize the possibility of biases in the results. The GCM has a latitudinal and longitudinal resolution of 0.94 by 1.25 degrees. The grid chosen to represent the study area and its selected meteorological stations is a 3 by 2 matrix (Figure 5). The centroids of the GCM grids

were interpolated via the inverse distance weighting (IDW) method to develop composite projected values for each of the meteorological stations as performed in similar studies as Li et al. (2012) and Guo et al. (2009).
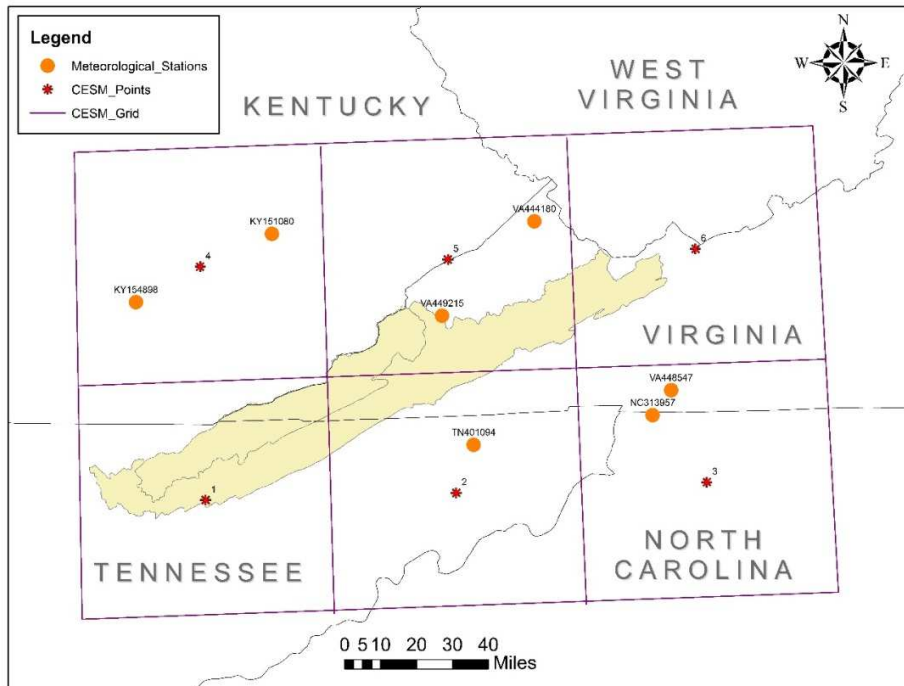
Figure 5. GCM Grid of CESM1.0

Optimization Model

Norris Reservoir's operation policy's flood and balancing guide lines were optimized through simulating the reservoir's hydrologic routing. The routing results were used as input into a conceptualized penalty function (or benefit function), yielding a penalty value defined in the Penalty Function and Optimization. Finally, an optimized reservoir operation policy was developed using the optimization model to minimize the penalty function.

Reservoir Routing Simulation

The hydrologic routing of Norris Reservoir was simulated using the runoff values generated by the combined model and an operational policy with the flow and elevation requirements acquired from TVA. Determination of reservoir elevation at a given time-step was performed utilizing the generated inflow hydrographs, the allowable outflow, and a Norris Reservoir stage-storage chart obtained from TVA (Figure 6). Initial storage was set at the current routing policy's balancing guide line, and storage was added monthly, based on the hydrologic mass balance of the reservoir that can be computed for a monthly time step *t* as:

$$S(t) = S_{t-1} + I_t - \sum O_{i,t} - W_t \tag{10}$$

$$for\ O_{min} \leq O_t \leq O_{max}\ and\ S_{min} \leq S_t \leq S_{max}$$

where S is the storage of the reservoir in MCM, I is monthly inflow in MCM, O is the monthly outflow in MCM, and W is the monthly withdrawal from the dam in MCM. The withdrawal (W) was assumed to be zero since there is no significant water withdrawal reported. Outflow were set per minimum requirements set by TVA; in which given a specific storage, the minimum outflow necessary to provide all available outflow requirements was used (Appendix 5). The final output for any time-step is the reservoir elevation in ft, which was obtained using the TVA acquired 1970 stage-storage-surface area diagram to convert from reservoir storage to dam elevation (Figure 6).
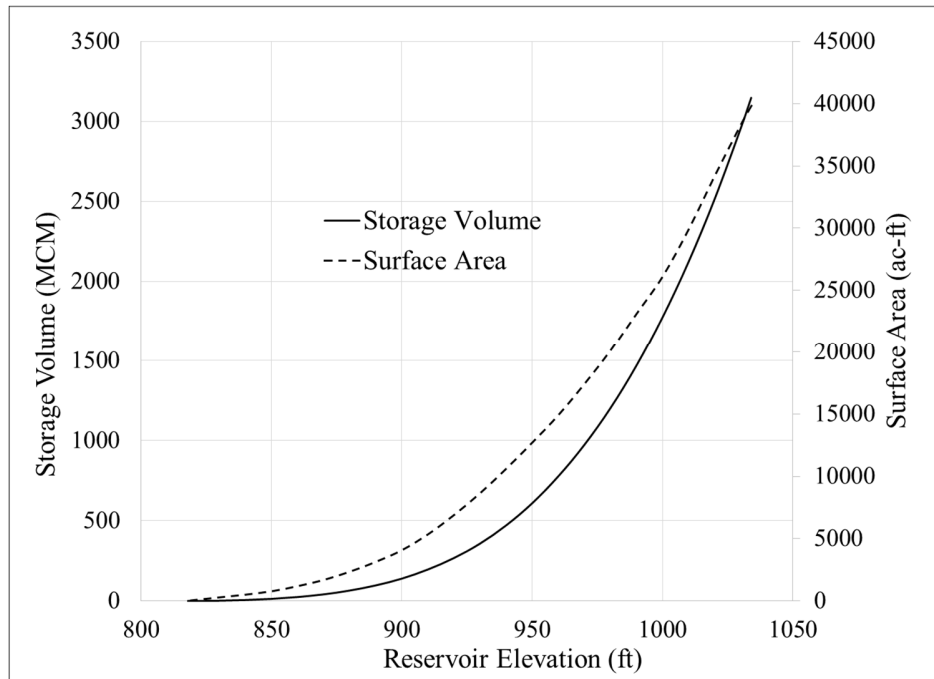
Figure 6. Stage-Storage-Surface Area Diagram from Norris Reservoir

Penalty Function and Optimization

The penalty function which the optimization model is minimizing, consists of five inflow and three outflow penalties. The values to meet specific requirements were obtained through consultation with TVA, based on their hierarchy of needs. A penalty was applied for any time step for which the penalty was broken. The five inflow penalties in order from least to highest penalty weight include:

1. Reservoir elevation above the flood guide (Figure 2).

2. Reservoir elevation below balancing guide (Figure 2).

3. Reservoir elevation above 1030 feet (historical high is 1030.38).

4. Reservoir elevation below 955 feet (unable to provide flow for navigation).

5. Reservoir elevation above 1034 feet (top of gate).

Figure 7 represents the weights of the varying elevation penalties, which presents that the penalty between the flood and balancing guide is a quadratic continuous function; while the remaining penalties are expressed as step functions which increase logarithmically at every threshold elevation (1000 for Penalty 3 and 4 and 10000 for Penalty 5).

The three outflow penalties in order from least to highest penalty weight include:

6. Inability to provide cooling requirement flows for Bull Run fossil plant (Appendix 5). A penalty value is incurred as 1000 per violation.

7. Inability to provide flows for ecosystem and hydropower generation requirements (Appendix 5). A penalty value is incurred as 10000 per violation.

8. Flow exceed maximum outflow to prevent flood inundation (1028 MCM). A penalty value is incurred as 10000 per violation.

Each set of inflow hydrograph will yield eight penalty values and they are summed to represent total penalty for each inflow. The operation policy was optimized by minimizing the average penalty value using 100 sets of inflow hydrograph data derived from Monte-Carlo simulations. This study compares the penalty values yielded by the current and revised policy (i.e., flood and balancing guide lines). This study used genetic algorithms (GAs), which are generally used to find a near global solution in complex error surface, with multiple decision variables. GAs are fundamentally search algorithms which use a Darwinian natural selection approach to perform a series of generations (iterations) consisting of selections, reproductions, and mutations to obtain an optimal solution (Wardlaw and Sharif 1999, Chen 2003, Cheng et al. 2008). A more in depth description of GAs, and its applications are available in Holland (1975) and Ross and Corne (1994). An example of a possible scenario for the penalty function is shown in Figure 7.
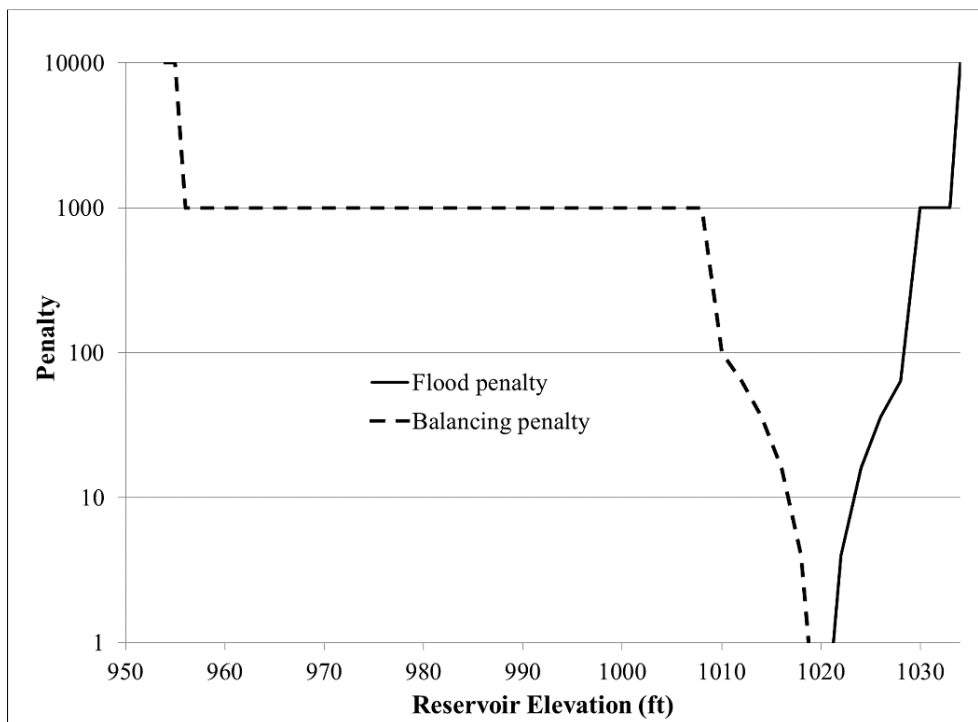
Figure 7. Conceptual Penalty Function of Reservoir Elevation for Optimization Model

CHAPTER III

RESULTS AND DISCUSSION

Generation of Composite Climate Data

Organization and Calculation of Composite GCM Data

The IDW interpolated composite GCM values for each meteorological station were used to develop composite projected values for the study area. This was completed by utilizing the same Thiessen weights used to interpolate the observed data. Appendix 2 and 3 visually present the change in temperature (°C) and precipitation (mm) from the GCM data to the observed data, respectively. It was noticed that the most significant variances in temperature laid in the winter months for all three GCM time spans, which showed an average annual change from the observed dataset of -0.42°C, 0.34°C, and 0.89°C for the time spans 2030's, 2050's, and 2070's, respectively. Also, historically the hottest month of the year, July, showed a decrease in temperature for all three scenarios. Finally, the GCM data indicating that the 2030's time span has an annual mean temperature 0.4°C lower than the observed dataset, led to the possible conclusion that this decrease in temperature is caused by increased precipitation and cloud cover during the summer months.

Visual representation of the results show increase in precipitation for most months (Appendix 3). Perturbations of 14.0, 18.27, and 19.9 percent for the time spans 2030's, 2050's, and 2070's were viewed from the observed data, respectively. It can also be seen that the perturbation in precipitation follows a temporally sinuous pattern. Therefore it was noted that the GCM predicts extreme flood and drought occurrences are to greatly increase in the future. Finally, there is an increase in average yearly precipitations of 13.0 mm, 17.2 mm, and 18.5 mm for time spans 2030's, 2050's, and 2070's, respectively.

To mitigate possible issues in projecting runoff posed by the variance from the observed to GCM data, the Conditional Generation Method (CGM) developed by Kim et al. (2008) was utilized to generate 100 instances of a 31-year time series, noted as "BASE" case (representing 1976~2006), from the observed hydro-climatic data. CGM was chosen due to its use in previous and relevant studies, and its ability to address hydro-climatic variability between successive months (Kim et al. 2008, Choi 2011). Once BASE was developed, 100 instances of 31-year time series for the 2030's, 2050's, and 2070's were developed based upon the perturbation and °C change from the observed data and raw GCM time span data. Precipitation and temperature results for comparison between the generated CGM data and observed data can be seen in Figure 8. From this table, it can be seen that the CGM generated precipitation and temperature data were very comparable to the historical data in both monthly means and standard deviation. This is due to CGM's ability to address both historical and temporal data by considering the conditional probability associated with the transition from successive months, and randomly selecting values for precipitation and temperature within the range of state for the month of concern.
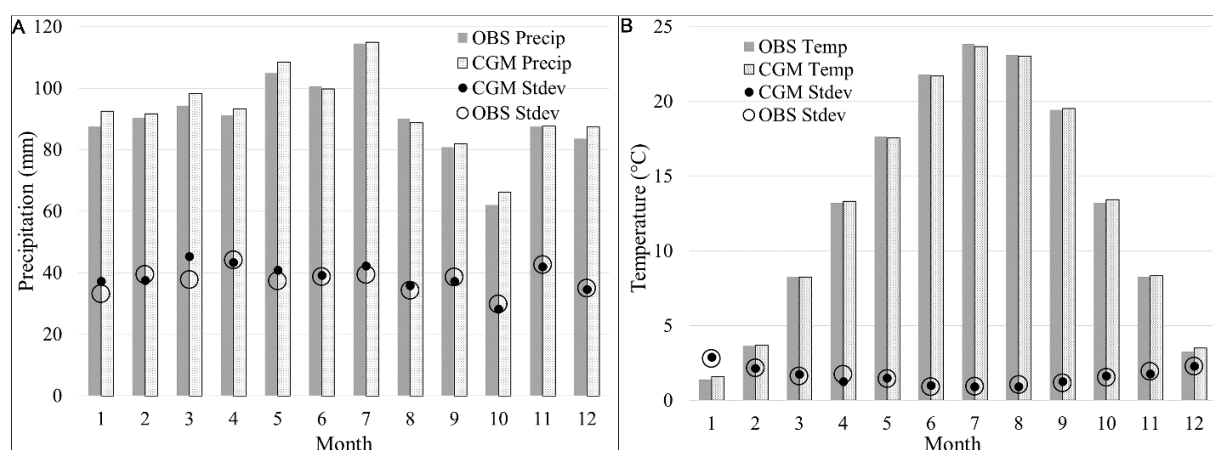
Figure 8. Comparison between the Observed and the Generated by CGM (A: Precipitation and B: Temperature)

Hydrologic Model Calibration

Variable Selection for MLR and ANN

The significant variables were selected via a forward stepwise regression, defined in the methods. Variables were chosen based on a p-value from the stepwise regression, which showed the statistical significance of how well the variable correlates with the output being predicted (Table 2). From Table 2 it can be seen that PET_t was rejected due to having a p-value of 0.81. From the test performed, any variable with a p-value greater than 0.05 is considered not significant. The variables which were not thrown out are to be used for the MLR and ANN models for the combined model construction. The Tank model uses only P_t and PET_t, because the model accounts for real-time soil moisture that is carried over from the previous time step as discussed in the Methods section.

Table 2. Results from Stepwise Regression

Variable	Coefficient	p-val
~~PET_t~~	~~-0.010~~	~~0.807~~
PET_{t-1}	-0.440	4.08e-64
P_t	0.474	1.24e-50
P_{t-1}	0.155	2.74e-08

Statistical Performance of the Selected Models

The weight given to each statistical model for the combined model is directly correlated to the ability of each model to predict the observed streamflow. The MLR was performed using a square root transformation to obtain better correlation. The results of the MLR analysis can be given in the equation below:

$$Q = \left(0.78 - 0.049 * \sqrt{PET_{t-1}} + 0.64 * \sqrt{P_t} + 0.27 * \sqrt{P_{t-1}}\right)^2 \tag{11}$$

Where Q is the monthly runoff in millimeters (mm), PET_{t-1} is the input potential evapotranspiration from a previous time-step (t-1) in mm, P_t is the input precipitation at time t in mm , and P_{t-1} is the precipitation at a previous time-step (t-1). The use of the square root transformation produced much more desired results, with an R^2 of 0.77.

The TANK model was calibrated and validated using the observed data which covered a 30 year span from 1977-2006. The 20 year span from 1977 to 1996 was used for calibration, and the remaining 10 years from 1997-2006 were used for validation. This resulted in a R^2 of 0.73.

The ANN model was performed using the same variables determined significant by the stepwise regression. The percent of observed data to be used for training, validation, and testing, were 90, 5, and 5 percent, respectively. These percentages were derived from multiple iterations of various subsample sizes to obtain the best overall performance. The R^2 for the ANN model was 0.81.

Proceeding the calibration and validation of all three models, eight-post processing tests were performed to determine the strengths of each model. The tests included evaluation of strength in model fitting via R^2, seasonality, annual runoff, high runoff season, low runoff season, low runoff events (observed runoff less than 10th percentile), high runoff events (observed runoff greater than 90th percentile), and median runoff (in between the 25th and 75th quartiles) via absolute error (Table 3).

From the analysis presented in Table 3, it can be seen that the MLR model more strongly predicted the annual runoff and low runoff events. The tank model's strength laid in predicting the low runoff season and high runoff events. Finally, the ANN model performed best at predicting

overall seasonality (total error), high runoff season, and runoff in between the 25th and 75th quartiles of the distribution.

Table 3. Strength Testing of Individual Models

Test	Equation	MLR	TANK	ANN	Combined Model
R^2 (Overall Prediction)	$= 1 - \sum_i \dfrac{(OBS_i - Modelled_i)^2}{(OBS_i - \overline{OBS})^2}$	0.77	0.73	0.81	0.80
Total Error (mm) (ABS Error)	$= \sum |OBS_t - Model_t|$	4545	5082	4093	4131
Annual Runoff Error (mm) (Full 30 yr Time Span)	$= |OBS_{annual} - Model_{annual}|$	19.49	37.16	28.54	17.68
High Runoff Season Error (Dec - May)	$= \sum_{Dec}^{May} \left| \dfrac{OBS_t - Model_t}{OBS_t} \right|$	1.17	1.09	0.93	0.99
Low Runoff Season Error (Jun - Nov)	$= \sum_{Jun}^{Nov} \left| \dfrac{OBS_t - Model_t}{OBS_t} \right|$	4.10	3.76	4.11	4.07
Low Runoff ABS Error (mm) ($< 10\%$ OBS Distribution)	$= \sum |OBS_t - Model_t|_{OBS<10\%}$	170	203	208	156
High Runoff ABS Error (mm) ($> 90\%$ OBS Distribution)	$= \sum |OBS_t - Model_t|_{OBS>90\%}$	1330	1044	1057	1142
25-75 Quartile ABS Error (mm) (50% OBS Distribution)	$= \sum |OBS_t - Model_t|_{25\%<OBS<75\%}$	1928	2574	1655	1734

Combined Model

The combined model was composed through linear programing (LP) coupling the three individual models with the objective function to yield the lowest prediction error (i.e., superior model performance than individual models), and the observed data utilizing the entire timespan.

The combined model produced an R^2 of 0.80, and adequately accounted for seasonality and extreme runoff. Appendix 4 represents a 5 year overlay plot of the observed data, individual models, and combined model output. Table 3 compares the strength test results of the combined model to the individual models. Although the combined model did not outperform every test, it can be seen that on average, the combined model had higher performance in all predictions tested except predicting flows above the 90th percentile.

Runoff Generation for GCM Data

CGM simulations perturbed by the GCM projections were used as input into the combined model to obtain runoff for each of the 30 year scenarios (BASE, 2030's, 2050's, and 2070's). To perform a visual assessment of the combined model output, the monthly arithmetic mean of 100 CGM simulations were taken, followed by the monthly arithmetic mean of 30 year time spans. Figure 9 presents the monthly arithmetic means runoff change of the projected scenarios to BASE. Average runoff was projected to increase throughout the entire year except for a decrease in February. All three scenarios showed increases in the spring and summer seasons of approximately 35 and 100 percent, respectively.
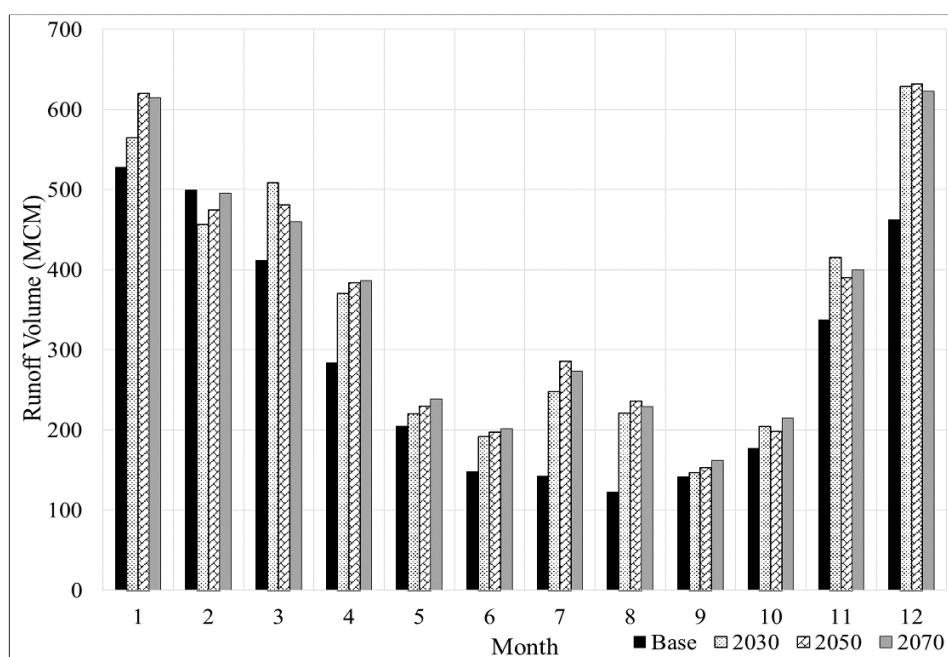
Figure 9. Mean Runoff for BASE and Projected Time Spans

It can be observed from Table 4 that in March and November the 2030's have the highest maximum runoff, and that the runoff for March was the highest runoff value for all three projected datasets. These results may be explained by Appendix 2 and 3, where these two time steps were located at points where the 2030's have a higher increase in precipitation or a greater decrease in temperature compared to the 2050's and 2070's. This can be explained by the extreme decrease in temperature, which greatly reduces the impact of potential evapotranspiration on the 2030's at that time step. The annual percent increase from BASE for the 2030's, 2050's and 2070's were 20.71, 23.78, and 24.33, respectively. This trend showed that although runoff had significantly increased by the 2030's, that by the 2070's the increase in runoff was beginning to level out.

Table 4. Statistics of Runoff Simulated for BASE and Future Time Spans

Unit: MCM

Month	Statistic	BASE	2030	2050	2070	Month	Statistic	BASE	2030	2050	2070
1	Mean	528.17	564.84	620.10	615.18	7	Mean	142.24	247.91	286.13	273.88
	Min	143.25	120.10	180.42	169.84		Min	22.52	36.93	40.28	38.57
	Max	1116.02	1219.36	1306.41	1299.83		Max	397.43	834.27	959.48	917.18
	Std Dev	197.08	204.01	224.50	229.01		Std Dev	67.32	152.34	183.31	173.21
2	Mean	499.28	456.10	474.71	495.40	8	Mean	122.34	221.17	236.04	229.06
	Min	106.50	95.64	100.77	99.69		Min	24.92	36.97	38.52	38.00
	Max	1209.59	1104.06	1173.76	1203.27		Max	378.56	773.32	829.23	821.93
	Std Dev	196.60	181.02	191.81	198.97		Std Dev	61.56	133.63	140.14	135.28
3	Mean	411.96	508.72	481.12	460.14	9	Mean	141.25	146.62	152.88	162.22
	Min	83.72	116.71	103.87	106.14		Min	37.92	37.74	39.84	38.71
	Max	1149.66	1348.93	1316.59	1277.08		Max	475.71	432.04	470.02	509.42
	Std Dev	205.81	261.55	251.35	239.35		Std Dev	84.60	73.38	79.09	85.27
4	Mean	283.44	370.47	384.09	386.68	10	Mean	177.33	204.72	198.03	215.24
	Min	39.44	47.34	51.00	41.16		Min	34.60	31.36	34.12	36.27
	Max	741.97	959.22	971.74	975.27		Max	551.17	666.97	639.49	701.58
	Std Dev	149.08	197.83	211.17	215.17		Std Dev	100.12	119.87	114.83	123.74
5	Mean	205.06	219.89	229.60	239.01	11	Mean	337.54	415.19	389.69	400.09
	Min	53.70	54.92	56.88	55.13		Min	42.88	48.78	47.61	52.06
	Max	576.03	612.92	650.04	711.94		Max	845.87	968.99	943.61	952.15
	Std Dev	103.85	107.22	116.29	122.41		Std Dev	188.12	217.72	212.25	214.55
6	Mean	147.99	191.50	197.58	201.27	12	Mean	462.69	628.62	632.01	622.91
	Min	25.31	35.95	31.19	32.17		Min	107.09	130.37	161.20	152.81
	Max	409.24	614.06	670.63	660.94		Max	940.07	1248.39	1267.42	1244.98
	Std Dev	76.87	117.38	122.59	125.13		Std Dev	170.47	226.25	235.58	231.47

Reservoir Routing and Optimization

Weighted penalty values were given in increasing magnitudes for deviation from the flood guide (Figure 2), this was performed to imitate one of TVA's primary objectives of maintaining reservoir elevation at the flood guide. Reservoir routing, using the combined model output as input, was calculated for each time-span using the current policy. Following, optimized policies altering the flood and balancing guide line elevations, were generated for each time-span using a genetic algorithm to minimize the average of the 100 Monte Carlo realizations summed penalty values. Performance of the optimization model was determined by comparing three scenarios, which are performance using 1) the current operation policy guide lines (Current), 2) the optimal operation policy determined from BASE (BASE_Opt), and 3) the optimized operation policy determined with respect to each future scenario (TS_Opt). A summary of the optimization and individualized penalty results are given in Tables 7 and 8, respectively.

BASE_Opt and TS_Opt policies both showed large decreases in penalties compared to the current policy (Table 5). The BASE_Opt scenario showed penalty decreases ranging from 22.2 to 24.4 percent, while the TS_Opt scenario showed ranges from 22.4 to 37.0.

Table 5. Optimization Model Results

year	ΔPenalty from Current to BASE_Opt (%)	ΔPenalty from Current to TS_Opt (%)
BASE	-22.4	-22.4
2030	-23.3	-35.4
2050	-22.2	-34.6
2070	-24.4	-37.0

Columns in Table 6 represent the individualized penalties assessed in this study. From Table 6, it is obvious that the routing penalties for both the BASE_Opt scenario and the relative TS_Opt scenarios showed significant decreases in individualized penalties when compared to the penalty produced by the current policy, especially for the third optimization method.

The decreases in penalties from Tables 5 and 6 can be explained by having higher runoff volumes, helping maintain the reservoir elevation at the Flood Guide. However, by emphasizing the reservoir elevation to be maintained at the flood guide, the penalty for not providing enough outflow for Bull Run slightly increased, and the penalty for preventing flooding downstream significantly increased for all scenarios except 2070's. This is best explained through the discussion of the occurrence of runoff events surpassing 90th and 95th percentile, this shoed that the 2070's scenario had less events surpassing these percentiles than the 2030's and 2050's. Moreover, this can be explained by the relative standard deviation of the 2070's scenario being less than the other two scenarios.

The results of the optimization model showed a decrease in the overall range between the flood and balancing guide elevations for all optimized scenarios except 2070's, which has a percent increase of 0.7 percent. It is also noted that the decrease in range was decreasing from one scenario to its chronologically successive scenario, and that this decrease was primarily caused through increasing the flood guide elevation. This can be explained by the fact that the results were derived from optimizing the projected scenarios based on the optimized BASE scenario. Therefore, since more runoff was being projected chronologically, it is logical that the range for each successive scenario's policy be increased. Figure 10 visually represents the differences in the current to the BASE optimized flood and balancing guide.

Table 6. Optimization Model Values for Individual Penalties

Year	Policy Test	Penalty 1 fld~bal	Penalty 2 >1030	Penalty 3 >1034	Penalty 4 <bal	Penalty 5 navi	Penalty 6 cooling	Penalty 7 eco/hydro	Penalty 8 fld_down	sum
BASE	Current	12451.62	0.00	0.00	35670.00	0.00	5460.00	0.00	0.00	53581.62
	BASE_Opt	6496.51	0.00	0.00	29610.00	0.00	5460.00	0.00	0.00	41566.51
	TS_Opt	6496.51	0.00	0.00	29610.00	0.00	5460.00	0.00	0.00	41566.51
2030	Current	10512.41	0.00	0.00	22120.00	0.00	6450.00	0.00	6700.00	45782.41
	BASE_Opt	5046.78	0.00	0.00	16940.00	0.00	6450.00	0.00	6700.00	35136.78
	TS_Opt	4348.93	0.00	0.00	12060.00	0.00	6450.00	0.00	6700.00	29558.93
2050	Current	10279.64	0.00	0.00	20880.00	0.00	7150.00	0.00	7000.00	45309.64
	BASE_Opt	4961.07	0.00	0.00	16130.00	0.00	7150.00	0.00	7000.00	35241.07
	TS_Opt	3661.93	0.00	0.00	11810.00	0.00	7150.00	0.00	7000.00	29621.93
2070	Current	10095.41	0.00	0.00	19770.00	0.00	6220.00	0.00	3400.00	39485.41
	BASE_Opt	4863.48	0.00	0.00	15350.00	0.00	6220.00	0.00	3400.00	29833.48
	TS_Opt	3756.85	0.00	0.00	11500.00	0.00	6220.00	0.00	3400.00	24876.85

Note: The penalties are defined as follows: 1) Reservoir Elevation being below the flood guide, but above the balancing guide; 2) Reservroi elevation being above 1030 ft; 3) Reservoir elevation being above 1034 ft; 4) Reservoir elevation being below the balancing guide; 5) Inability for reservoir to provide minimum outflow required for navigation; 6) Inability for reservoir to provide minimum outflow required for Bull Run Fossil Plant cooling; 7) Inability for reservoir to provide minimum outflow required for hydropower generation and ecosystem 8)Inability for reservoir to prevent flooding down stream.
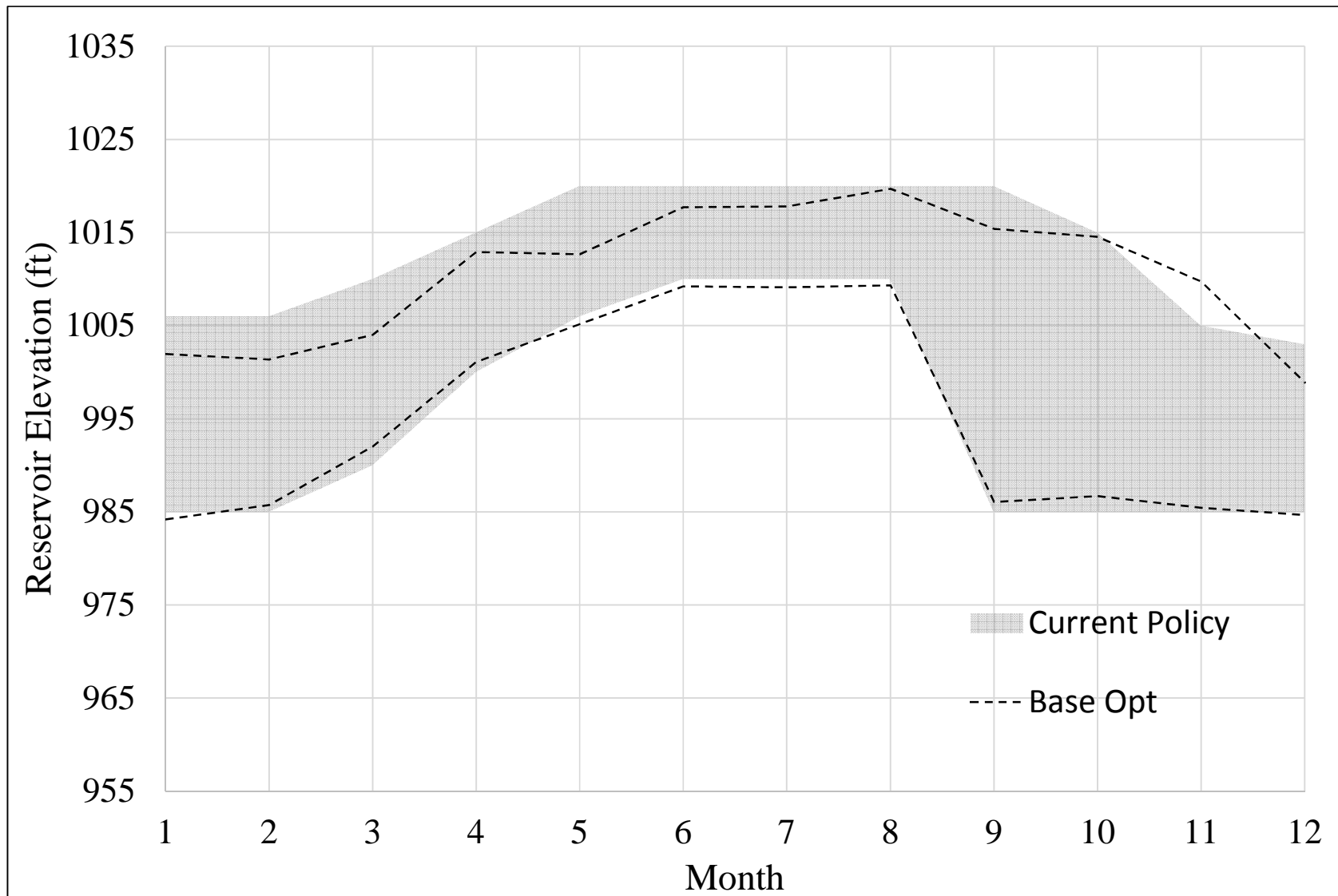
Figure 10. BASE Optimized Policy Overlaying Current Policy

CHAPTER IV

CONCLUSIONS AND RECOMMENDATIONS

This study aimed to assess the potential impacts of climate change on the performance Norris Reservoir for three timespans, 2030's, 2050's, and 2070's, and optimize their current policy flood and balancing guide lines to be better equipped for handling these impacts.

The key findings of this study include:

1. The GCM data used, revealing increases in annual precipitation with warmer winters and cooler summers, resulted in increased runoff by up to 24.3% for Norris Reservoir by 2070.

2. The use of a linearly programmed combined hydrologic model proved to be more sufficient in estimating a wider range of runoff values than any of the individual hydrologic models could independently, regardless of the combined model having a slightly lower R^2 than the ANN model.

3. Although the current policy was able to handle the higher inflow, the generated penalties were greatly decreased through the use of a genetic algorithm driven optimization model. The results could be attributed to the increased inflow for Norris Reservoir, enabling the maintenance of reservoir elevation at the flood guide line to be more easily accomplished; although, this increased the risk for flooding downstream.

In conclusion, for a reservoir that works within a network, an increase of runoff in the entire system may pose many threats unexplored by this study. Therefore, it is recommended that future studies consider encompassing the entire TVA system, and that temporal resolution be

increased to a daily time-step, instead of monthly, to account for extreme events. This will allow the ability to work more closely with TVA, helping to better define the penalty function, more accurately account for the reservoir network process, and compare the combined hydrologic model with the TVA SAC-SMA model. Moreover, the results produced could also be attributed to the GCM used. Due to the uncertainty and variance from one GCM to the next, it is recommended that a wide variety of GCMs, and RCPs scenarios, be taken into consideration.

LIST OF REFERENCES

Allen, M. R. and W. J. Ingram (2002). "Constraints on future changes in climate and the hydrologic cycle." Nature 419(6903): 224-232.

Amatya, D., R. Skaggs and J. Gregory (1997). "Evaluation of a watershed scale forest hydrologic model." Agricultural water management 32(3): 239-258.

Anderegg, W. R., J. W. Prall, J. Harold and S. H. Schneider (2010). "Expert credibility in climate change." Proceedings of the National Academy of Sciences 107(27): 12107-12109.

Andersson, L., J. Wilk, M. C. Todd, D. A. Hughes, A. Earle, D. Kniveton, R. Layberry and H. H. Savenije (2006). "Impact of climate change and development scenarios on flow patterns in the Okavango River." Journal of Hydrology 331(1): 43-57.

Arnell, N. W. (1999). "Climate change and global water resources." Global environmental change 9: S31-S49.

Askew, A. (1987). "Climate change and water resources." The Influence of Climate Change and Climatic Variability on the Hydrologic Regime and Water Resources 168: 421-430.

Beale, Mark, Martin T. Hagan, and Howard B. Demuth. "Neural network toolbox." Neural Network Toolbox, The Math Works (2014).

Bell, J. L., L. C. Sloan and M. A. Snyder (2004). "Regional changes in extreme climatic events: A future climate scenario." Journal of Climate 17(1).

Black, P. E. (2007). "Revisiting the Thornthwaite and Mather Water Balance1."Journal of the American Water Resources Association 43(6): 1604-1605.

Boughton, W. and F. Chiew (2007). "Estimating runoff in ungauged catchments from rainfall, PET and the AWBM model." Environmental Modelling & Software 22(4): 476-487.

Buytaert, W., R. Celleri, P. Willems, B. D. Bièvre and G. Wyseure (2006). "Spatial and temporal rainfall variability in mountainous areas: A case study from the south Ecuadorian Andes." Journal of Hydrology 329(3): 413-421.

Chang, F.-J. and Y.-T. Chang (2006). "Adaptive neuro-fuzzy inference system for prediction of water level in reservoir." Advances in Water Resources 29(1): 1-10.

Chang, F.-J. and Y.-C. Chen (2001). "A counterpropagation fuzzy-neural network modeling approach to real time streamflow prediction." Journal of Hydrology 245(1): 153-164.

Chaubey, I., C. Haan, J. Salisbury and S. Grunwald (1999). "Quantifying Model Output Uncertainty due to Spatial Variability of Rainfall."Journal of the American Water Resources Association 35(5): 1113-1123.

Chen, L. (2003). "Real Coded Genetic Algorithm Optimization of Long Term Reservoir Operation."Journal of the American Water Resources Association 39(5): 1157-1165.

Chen, R.S., L. C. Pi and C. C. Hsieh (2005). "Application of Parameter Optimization Method for Calibrating Tank Model."Journal of the American Water Resources Association 41(2): 389-402.

Cheng, C.-T., W.-C. Wang, D.-M. Xu and K. Chau (2008). "Optimizing hydropower reservoir operation using hybrid genetic algorithm and chaos." Water Resources Management 22(7): 895-909.

Choi, Y.-G. (2011). Potential Impacts of Climate Change on Water Resources and Water Quality of Norris Lake, Tennessee. Master's Thesis, University of Tennessee.

Christensen, N. S., A. W. Wood, N. Voisin, D. P. Lettenmaier and R. N. Palmer (2004). "The effects of climate change on the hydrology and water resources of the Colorado River basin." Climatic Change 62(1-3): 337-363.

Cooper, V., V.-T.-V. Nguyen and J. Nicell (2007). "Calibration of conceptual rainfall–runoff models using global optimisation methods with hydrologic process-based parameter constraints." Journal of Hydrology 334(3): 455-466.

Cruff, R. (1967). "comparison of methods of estimating potential evapotranspiration from climatological data in arid and subhumid environments."

Dawson, C. and R. Wilby (2001). "Hydrological modelling using artificial neural networks." Progress in Physical Geography 25(1): 80-108.

Demuth, H., M. Beale and M. Hagan (2008). "Neural network toolbox™ 6." User's guide.

Dingman, S. (2002). Water in soils: infiltration and redistribution. Physical hydrology, upper saddle river, New Jersey: Prentice-Hall, Inc: 645.

Easterling, D. R., G. A. Meehl, C. Parmesan, S. A. Changnon, T. R. Karl and L. O. Mearns (2000). "Climate extremes: observations, modeling, and impacts." science 289(5487): 2068-2074.

Elshamy, M. E., I. A. Seierstad and A. Sorteberg (2009). "Impacts of climate change on Blue Nile flows using bias-corrected GCM scenarios." Hydrology & Earth System Sciences 13(5).

Federer, C., C. Vörösmarty and B. Fekete (1996). "Intercomparison of methods for calculating potential evaporation in regional and global water balance models." Water Resources Research 32(7): 2315-2321.

Frederick, K. D. and D. C. Major (1997). "Climate change and water resources." Climatic Change 37(1): 7-23.

Gao, Y., J. Fu, J. Drake, Y. Liu and J. Lamarque (2012). "Projected changes of extreme weather events in the eastern United States based on a high resolution climate modeling system." Environmental Research Letters 7(4): 044025.

Gleckler, P. J., K. E. Taylor and C. Doutriaux (2008). "Performance metrics for climate models." Journal of Geophysical Research: Atmospheres (1984–2012) 113(D6).

Guegan M., K. Madani, and C. B. Uvo. 2012. Climate Change Effects on the High-Elevation Hydropower System with Consideration of Warming Impacts on Electricity Demand and Pricing. California Energy Commission. Publication number: CEC-500-2012-020.

Guo, S., Guo, J., Zhang, J., & Chen, H. (2009). VIC distributed hydrological model to predict climate change impact in the Hanjiang Basin. *Science in China Series E: Technological Sciences*, *52*(11), 3234-3239.

Haan, C. T., B. J. Barfield and J. C. Hayes (1994). Design hydrology and sedimentology for small catchments, Elsevier.

Hamlet, A. F. and D. P. Lettenmaier (1999). "Effects of Climate Change on Hydrology and Water Resources in the Columbia River Basin."Journal of the American Water Resources Association 35(6): 1597-1623.

Helton, J. C., J. D. Johnson, C. J. Sallaberry and C. B. Storlie (2006). "Survey of sampling-based methods for uncertainty and sensitivity analysis." Reliability Engineering & System Safety 91(10): 1175-1209.

Heuvelmans, G., B. Muys and J. Feyen (2006). "Regionalisation of the parameters of a hydrological model: Comparison of linear regression models with artificial neural nets." Journal of Hydrology 319(1): 245-265.

Holland, J. H. (1975). Adaptation in natural and artificial systems: An introductory analysis with applications to biology, control, and artificial intelligence, U Michigan Press.

IPCC (2013). Climate Change 2013: The Physical Science Basis. Contribution of Working Group I to the Fifth Assessment Report of the Intergovernmental Panel on Climate Change. T. F. Stocker, D. Qin, G.-K. Plattner, M. Tignor, S.K. Allen, J. Boschung, A. Nauels, Y. Xia, V. Bex and P.M. Midgley. Cambridge University Press, Cambridge, United Kingdom and New York, NY, USA: 1535.

Jain, S. (1993). "Calibration of conceptual models for rainfall-runoff simulation." Hydrological sciences journal 38(5): 431-441.

Karl, T. R., J. M. Melillo and T. C. Peterson (2009). Global climate change impacts in the United States, Cambridge University Press.

Kessel, D. G. (2000). "Global warming—facts, assessment, countermeasures." Journal of Petroleum Science and Engineering 26(1): 157-168.

Kim, U. and J. J Kaluarachchi (2008). "Application of parameter estimation and regionalization methodologies to ungauged basins of the upper Blue Nile River Basin, Ethiopia." Journal of Hydrology 362(1-2): 39-56.

Kim, U. and J. J. Kaluarachchi (2009). "Climate Change Impacts on Water Resources in the Upper Blue Nile River Basin, Ethiopia1."Journal of the American Water Resources Association 45(6): 1361-1378.

Kim, U., J. J. Kaluarachchi and V. U. Smakhtin (2008). "Generation of monthly precipitation under climate change for the upper blue Nile river basin, Ethiopia1."Journal of the American Water Resources Association 44(5): 1231-1247.

Kişi, Ö. (2007). "Streamflow forecasting using different artificial neural network algorithms." Journal of Hydrologic Engineering 12(5): 532-539.

Kişi, Ö. (2008). "River flow forecasting and estimation using different artificial neural network techniques." Hydrology Research 39(1).

Knutti, R., R. Furrer, C. Tebaldi, J. Cermak and G. A. Meehl (2010). "Challenges in combining projections from multiple climate models." Journal of Climate 23(10).

Lee, J.-Y. and B. Wang (2014). "Future change of global monsoon in the CMIP5." Climate Dynamics 42(1-2): 101-119.

Lee, S.-Y., A. F. Hamlet, C. J. Fitzgerald and S. J. Burges (2009). "Optimized flood control in the Columbia River Basin for a global warming scenario." Journal of water resources planning and management 135(6): 440-450.

Li, Zhi, Fen-Li Zheng, and Wen-Zhao Liu. "Spatiotemporal characteristics of reference evapotranspiration during 1961–2009 and its projected changes during 2011–2099 on the Loess Plateau of China." Agricultural and Forest Meteorology 154 (2012): 147-155.

Lu, J., G. Sun, S. G. McNulty and D. M. Amatya (2005). "A Comparison of Six Potential Evapotranspiration Methods for Regional Use in the Southeastern United States."Journal of the American Water Resources Association 41(3): 621-633.

Markoff, M. S. and A. C. Cullen (2008). "Impact of climate change on Pacific Northwest hydropower." Climatic Change 87(3-4): 451-469.

McCabe, G. J. and D. M. Wolock (1992). "Sensitivity of Irrigation Demand in a Humid-Temperature Region to Hypothetical Climatic Change."Journal of the American Water Resources Association 28(3): 535-543.

Meehl, G. A., J. M. Arblaster and C. Tebaldi (2005). "Understanding future patterns of increased precipitation intensity in climate model simulations." Geophysical Research Letters 32(18).

Meehl, G. A., W. M. Washington, W. D. Collins, J. M. Arblaster, A. Hu, L. E. Buja, W. G. Strand and H. Teng (2005). "How much more global warming and sea level rise?" science 307(5716): 1769-1772.

Morrison, J., M. C. Quick and M. G. Foreman (2002). "Climate change in the Fraser River watershed: flow and temperature projections." Journal of Hydrology 263(1): 230-244.

Mosner, M. S. and B. T. Aulenbach (2003). "Comparison of methods used to estimate lake evaporation for a water budget of Lake Seminole, southwestern Georgia and northwestern Florida."

Moss, R. H., J. A. Edmonds, K. A. Hibbard, M. R. Manning, S. K. Rose, D. P. Van Vuuren, T. R. Carter, S. Emori, M. Kainuma and T. Kram (2010). "The next generation of scenarios for climate change research and assessment." Nature 463(7282): 747-756.

Muleta, M. K. and J. W. Nicklow (2005). "Sensitivity and uncertainty analysis coupled with automatic calibration for a distributed watershed model." Journal of Hydrology 306(1): 127-145.

Palmer, W. C. and A. V. Havens (1958). "A graphical technique for determining evapotranspiration by the Thornthwaite method." Monthly Weather Review 86(4): 123-128.

Parajka, J., R. Merz and G. Blöschl (2005). "A comparison of regionalisation methods for catchment model parameters." Hydrology & Earth System Sciences Discussions 2(2).

Parker, J. M. (2008). The Influence of Hydrological Patterns on Brook Trout (Salvelinus fontinalis) and Rainbow Trout (Oncorhynchus mykiss) Population Dynamics in the Great Smoky Mountains National Park, University of Tennessee.

Parker, J. M. (2008). The influence of hydrological patterns on brook trout (Salvelinus fontinalis) and rainbow trout (Oncorhynchus mykiss) population dynamics in the Great Smoky Mountains National Park.

Payne, J. T., A. W. Wood, A. F. Hamlet, R. N. Palmer and D. P. Lettenmaier (2004). "Mitigating the effects of climate change on the water resources of the Columbia River basin." Climatic Change 62(1-3): 233-256.

Rani, D. and M. M. Moreira (2010). "Simulation–optimization modeling: a survey and potential application in reservoir systems operation." Water Resources Management 24(6): 1107-1138.

Ross, P. and D. Corne (1994). "Applications of genetic algorithms." AISB Quaterly on Evolutionary Computation 89: 23-30.

Seelbach, P. W., L. C. Hinz, M. J. Wiley and A. R. Cooper (2011). "Use of multiple linear regression to estimate flow regimes for all rivers across Illinois, Michigan, and Wisconsin." Fisheries Research Rep 2095: 1-35.

Shamseldin, A. Y. (1997). "Application of a neural network technique to rainfall-runoff modelling." Journal of Hydrology 199(3): 272-294.

Shamseldin, A. Y., K. M. O'Connor and G. Liang (1997). "Methods for combining the outputs of different rainfall-runoff models." Journal of Hydrology 197(1-4): 203-229.

Stone, M. C., R. H. Hotchkiss, C. M. Hubbard, T. A. Fontaine, L. O. Mearns and J. G. Arnold (2001). "Impacts of Climate Change on Missouri RWER Basin Water Yield."Journal of the American Water Resources Association 37(5): 1119-1129.

Sugawara, M., 1967. The flood forecasting by a series storage type model. International Symposium on Floods and Their Computation. August 1967, Leningrad, USSR.

Taylor, K. E., V. Balaji, S. Hankin, M. Juckes, B. Lawrence and S. Pascoe (2010). CMIP5 Data Reference Syntax (DRS) and Controlled Vocabularies.

Taylor, K. E., R. J. Stouffer and G. A. Meehl (2012). "An Overview of CMIP5 and the Experiment Design." Bulletin of the American Meteorological Society 93(4).

Tennessee Department of Energy and Conservation (TDEC) (2007). "Watershed Water Quality Management Plan for Powell River Watershed."

Tennessee Department of Energy and Conservation (TDEC) (2007). "Watershed Water Quality Management Plan for Upper Clinch River Watershed."

Tennessee Valley Authority (TVA) (1940). A Comprehensive Report on the Planning Design, Construction, and Initial Operations of the Tennessee Valley Authority's First Water Control Project. The Norris Project Technical Report. No. 1: 840.

Tennessee Valley Authority (TVA) (2004). Final Programmatic Environmental Statement - Tennessee Valley Authority Reservoir Operations Study, Tennessee Valley Authority (TVA).

Tennessee Valley Authority (TVA) (2006). TVA Reservoir Operations Study Wetland Monitoring Summary Report, Tennessee Valley Authority (TVA).

Tennessee Valley Authority (TVA) (2014). "Norris Reservoir." From http://www.tva.gov/sites/norris.htm.

Thomson, A. M., K. V. Calvin, S. J. Smith, G. P. Kyle, A. Volke, P. Patel, S. Delgado-Arias, B. Bond-Lamberty, M. A. Wise and L. E. Clarke (2011). "RCP4. 5: a pathway for stabilization of radiative forcing by 2100." Climatic Change 109(1-2): 77-94.

Thornthwaite, C. W. (1948). "An approach toward a rational classification of climate." Geographical review 38(1): 55-94.

Tokar, A. S. and P. A. Johnson (1999). "Rainfall-runoff modeling using artificial neural networks." Journal of Hydrologic Engineering 4(3): 232-239.

United States Environmental Protection Agency (EPA) (2002). Clinch and Powell Valley watershed ecological risk assessment. Washington, DC, National Center of Environmental Assessment. EPA/600/R-01/050.

United States Geological Survey (USGS) (2013). "Upper Clinch." from http://water.usgs.gov/lookup/getwatershed?06010205/www/cgi-bin/lookup/getwatershed.

Wagener, T. and H. S. Wheater (2006). "Parameter estimation and regionalization for continuous rainfall-runoff models including uncertainty." Journal of Hydrology 320(1): 132-154.

Wardlaw, R. and M. Sharif (1999). "Evaluation of genetic algorithms for optimal reservoir system operation." Journal of water resources planning and management 125(1): 25-33.

Watanabe, S., K. Sudo, T. Nagashima, T. Takemura, H. Kawase and T. Nozawa (2011). "Future projections of surface UV-B in a changing climate." Journal of Geophysical Research: Atmospheres (1984–2012) 116(D16).

World Meteorological Organization (WMO) (2013). WMO statement on the status of the global climate in 2012. WMO-No. 1108.

Wu, J., Y. Zhou, Y. Gao, J. S. Fu, B. A. Johnson, C. Huang, Y.-M. Kim and Y. Liu (2014). "Estimation and uncertainty analysis of impacts of future heat waves on mortality in the eastern United States." Environmental health perspectives 122(1): 10.

Xu, C.-y. (1999). "From GCMs to river flow: a review of downscaling methods and hydrologic modelling approaches." Progress in Physical Geography 23(2): 229-249.

Xu, C. Y. and V. Singh (2001). "Evaluation and generalization of temperature-based methods for calculating evaporation." Hydrological processes 15(2): 305-319.

Yokoo, Y., S. Kazama, M. Sawamoto and H. Nishimura (2001). "Regionalization of lumped water balance model parameters based on multiple regression." Journal of Hydrology 246(1): 209-222.

Zealand, C. M., D. H. Burn and S. P. Simonovic (1999). "Short term streamflow forecasting using artificial neural networks." Journal of Hydrology 214(1): 32-48.
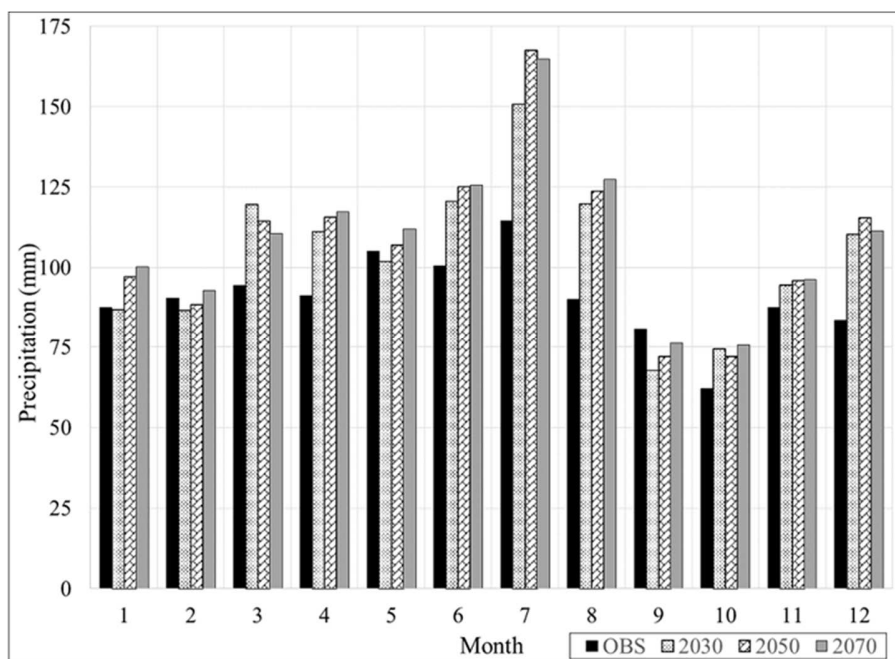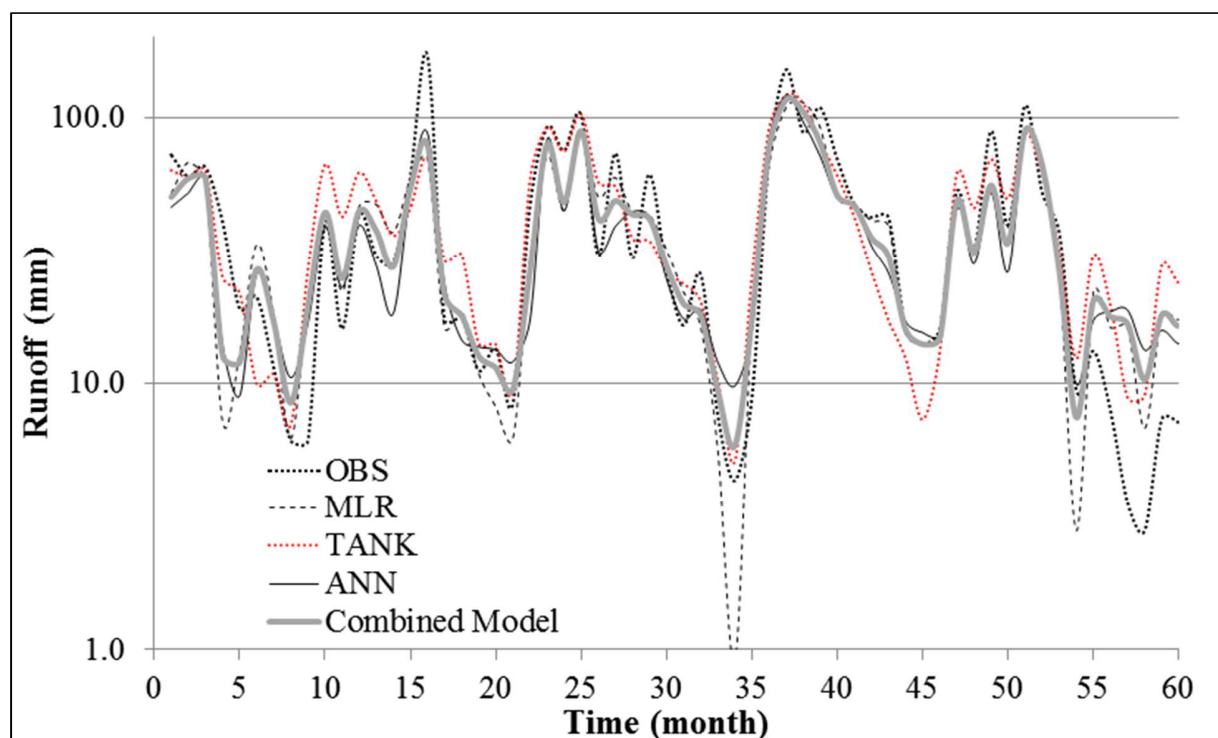
APPENDIX

Appendix 1: Norris Dam (http://www.tva.gov/sites/norris.htm)
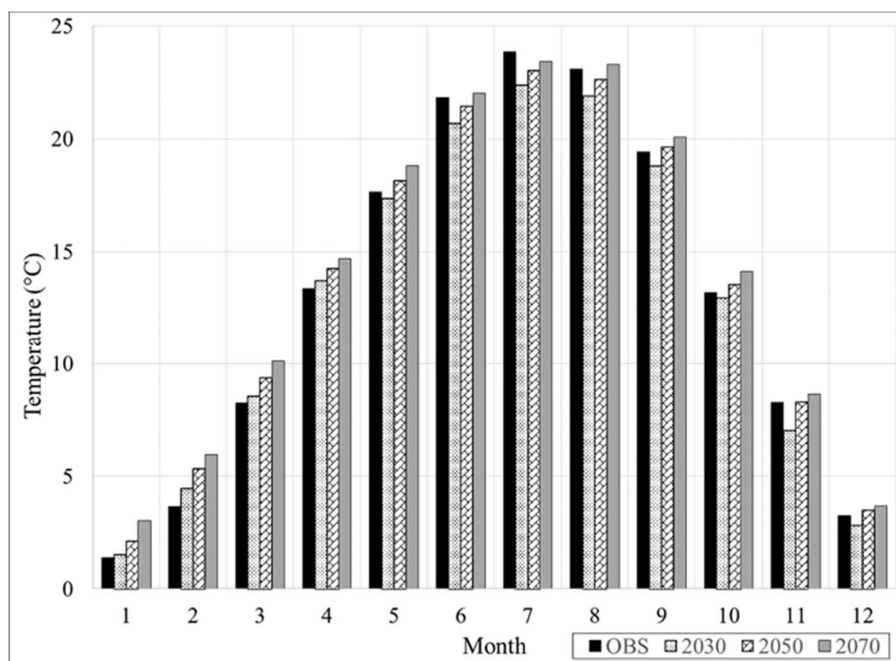
Appendix 2: Mean Temperature for Observed and Projected Time Spans

Appendix 3: Mean Precipitation for Observed and Projected Time Spans

Appendix 4: Runoff Simulation Accuracy from All Models to Observed Data

Appendix 5: Minimum Outflow Constraints for Norris Reservoir (MCM per month)

Month	Cooling minimum	Hydro-power and Ecosystem minimum
1	45.51	18.96
2	54.8	18.96
3	60.68	18.96
4	73.4	18.96
5	75.84	18.96
6	88.08	18.96
7	113.77	18.96
8	113.77	18.96
9	110.1	18.96
10	151.69	18.96
11	44.04	18.96
12	45.51	18.96

VITA

Joseph P. Rungee was raised in Murfreesboro, Tennessee. He attended Siegel High School and graduated in May of 2008. After graduating from high school, Joseph enrolled into the University of Tennessee, Knoxville where he graduated with a Bachelor's of Science Degree in Civil and Environmental Engineering in December of 2012. Post-graduation, Joseph received a Graduate Research Assistantship at the University of Tennessee, Knoxville in the Civil and Environmental Engineering Department. After completing the required coursework, and fulfilling his research obligations, Joseph received his Masters of Science Degree in Environmental Engineering with a concentration in Water Resources in May of 2014.